International Journal of Modern Physics C

Computer model of biopolymer crystal growth and aggregation by addition of macromolecular units - a comparative study

J. Siódmiak*, A. Gadomski

Institute of Mathematics and Physics, University of Technology and Agriculture, 85-796 Bydgoszcz, Poland
**siedem@atr.bydgoszcz.pl*

Received Day Month Year
Revised Day Month Year

We discuss the results of a computer simulation of the biopolymer crystal growth and aggregation based on the 2D lattice Monte Carlo technique and the HP approximation of the biopolymers. As a modeled molecule (growth unit) we comparatively consider the previously studied non-mutant lysozyme protein, Protein Data Bank (PDB) ID: 193L, which forms, under a certain set of thermodynamic-kinetic conditions, the tetragonal crystals, and an amyloidogenic variant of the lysozyme, PDB ID: 1LYY, which is known as fibril-yielding and prone-to-aggregation agent. In our model, the site-dependent attachment, detachment and migration processes are involved. The probability of growth unit motion, attachment and detachment to/from the crystal surface are assumed to be proportional to the orientational factor representing the anisotropy of the molecule. Working within a two-dimensional representation of the truly three-dimensional process, we also consider that the crystal grows in a spiral way, whereby one or more screw dislocations on the crystal surface give rise to a terrace. We interpret the obtained results in terms of known models of crystal growth and aggregation such as B-C-F (Burton-Cabrera-Frank) dislocation driven growth and M-S (Mullins-Sekerka) instability concept, with stochastic aspects supplementing the latter. We argue the conditions under which crystals *vs* non-crystalline protein aggregates appear, and how the process depends upon difference in chemical structure of the protein molecule seen as the main building block of the elementary crystal cell.

Keywords: protein; lysozyme; MC simulation; HP model; coarse-graining; non-Kossel crystal; spiral growth.

PACS Nos.: 02.50.Ng, 68.35.Bs, 81.10.-h, 87.15.Kg, 87.15.Nn

1. Introduction

Physical computation becomes nowadays a useful tool/method in soft-matter physics, especially in protein science[1]. The Protein Data Bank (PDB) is the worldwide repository of 3D structure data of large molecules of proteins and nucleic acids. Most of the 3D macromolecular structure data in the PDB were obtained by one of three methods: X-ray crystallography, solution nuclear magnetic resonance (NMR) or theoretical modeling[2]. The first two are experimental methods. The empirical results of these methods accurately describe the 3D structure of the molecule in

the state in which measurements were taken. However, crystallization sometimes distorts portions of a structure due to contacts between neighboring molecules in the crystal. Still, protein crystals as used for diffraction studies are highly hydrated ("wet and gelatinous"), so structures determined from crystals are not much different from the structures of soluble proteins in aqueous solution. For these reasons we have chosen the lysozyme[a] for our modeling which forms under a certain set of conditions the tetragonal crystals.

Everyone of globular proteins has a more or less unique folded structure, which is determined by the sequence of amino-acids but which can change upon aggregation. Prediction of the folded structure of the given amino-acid sequence is a very important and still unsolved problem[3,4,5]. The purpose of simplified models such as the HP model, first introduced by Larson et al.[6] for surfactant-containing systems, and then successfully applied by Dill[3] to describe conformational behavior of lattice proteins, is not to make structure predictions, but rather to gain insights into the physical principles of folding and aggregation[5]. (Another important class of lattice models, involving the protein dynamics in a fairly coarse-grained way, with a special emphasis put on the potentials and forces between the monomers, is that of Go type, often realized by molecular dynamics, cf. Refs. [5, 1] and refs therein.) The HP model has only two types of amino-acids, hydrophobic (H) and hydrophilic/polar (P), instead of 20. The chain is modeled as a self-avoiding walk (SAW) on a 2D square lattice. HP model deals with proteins equipped with hydrophobic cores (as seen experimentally) that fold below a certain temperature, see Ref. [4] and refs therein. Because the HP procedure significantly simplifies real protein we will call it here a first-stage coarse-graining procedure. It enables to use HP model with its onto-cube-walls projected HP-properties, with a special emphasis placed on the outer region (skin) of the protein, which is the key feature of the proposed systematic coarse-graining procedure to be applied in the present work for a lysozyme biomolecule, but virtually, for any biomolecule[5]. The second level of the coarse-graining is seen when going from a (realizable) 3D domain to its (virtual) 2D equivalent: this is the core of the coarse-graining procedure offered in this paper named hereafter the second-stage coarse-graining. Its reliability (in the authors' opinion) is strongly supported by the spiral model of the crystal growth[7,8,9] (see Figure 1). The spiral model tells us that although the growing process is unquestionably a 3D process, it can, without losing of generality, be split into either its vertical or its horizontal sub-levels, and from the growing point of view the vertical cross-section[9], that we approach in our study, properly reflects the main properties and tendencies of the growth process and therefore deserves careful investigation.

There is a good number of analytical models that although they lead to very interesting results, usually cannot see the microscopic effects. Therefore, there is a need to support them with numerical calculations and computer simulations[1]. Most of

[a]Lysozyme is a small protein that attacks the protective cell walls of bacteria. It was the first enzyme ever to have its structure solved.

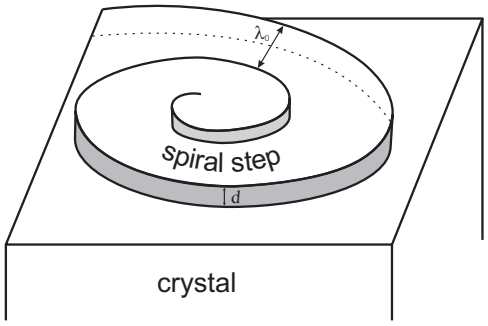

Fig. 1. A cartoon of the spiral growth of a crystal surface growing from solution - the B-C-F-type of growth[8,7]. The spiral is conducted by the screw dislocation center and becomes roughly equivalent to concentric circuit steps of height d with a separation distance λ_0, cf. Table 1.

the calculations/simulations presented so far[10,11,12] are not perceived as readily arising from the experiments but rather as interpreting/supporting those experiments. That is why our model gives advantage prior to those others mentioned[10,13] since it directly starts from a protein data resource and after resorting to the coarse-graining procedures mentioned, offers, for a chemically-limited choice of the two relevant (attachment/detachment) probabilities, a novel result of the otherwise defined as hydrodynamically favorable[14] constant tempo, V_{gr}, of the process. Outside this range of probability values the problem enters a nonlinear (nonstationary) hydrodynamic regime of the growing mode, also observed frequently in the experiment[15].
The organization of the present study is as follows In section 2, we present a computer model in which the growth unit preparation basis of the HP model for both variants of lysozyme (Subsection 2.1) and nucleus' preparation basis of the structure with minimum energy of the unit cell of the non-Kossel crystal[16] are described (Subsection 2.2), and finally the growth procedure is outlined (Subsection 2.3). In Section 3, we present a method of calculation of the growth rate in a direction normal to the surface of the growing structure. Section 4 presents some results of the simulation and comparison to the experiment. Finally, in Section 5 conclusions and final remarks are included.

2. PDB-based computer model

2.1. *Non-mutant and mutant growth unit preparation*

The simulation begins at an atomic-level analysis of the protein molecules under study, as taken from the Protein Data Bank. First, we appropriately reorient in space both molecules to obtain a satisfactory comparative arrangement. Next, we vertically locate molecules in the space. Such an orientation is characteristic of lysozyme molecules in a crystal of tetragonal form[16]. Once the orientation has succeeded, we prepare the 3D HP representation of the selected molecules[17]. We average over the coordinates of all atoms within one amino-acid and attribute hydrophilicity P

(-phobicity H)[18] to such prepared (averaged) monomers (see Figure 2a). Because the molecules are flexible and interact through the surface, we assume that the interaction takes place as if it were within the protein skin the thickness of which is taken to be equal to 25% of the molecule radius (see Figure 2b). Such 'isolated peelings' of the protein molecule are projected on the walls of the virtual cubic box, surrounding the protein (like a pumping up balloon in a cubic box). Next, we count how many H-type and P-type monomers appear on each wall of our box. The excess in a number of one of the monomer types (H or P) unambiguously determines the type of the wall of the surrounding box (see Figure 2c). In a next step, we select the direction of observation and we neglect the front and the rear side of the box because these walls, in a case of non-mutant growth unit, are devoid of the H-type monomers and the number of P-type monomers is the same for both sides. For the mutant, in turn, the situation is slightly different, see explanations below. Assuming that the P-type monomers do not interact with each other, we can say that these sides are non-reactive, so their contribution to "global" energy is equal to zero and this contribution can be neglected. The 2D square created in such a way is the growth unit with every side of P-type (see Figure 2d). The growth unit presented in Figure 2d will be called A-type. B-type arises from clockwise rotation of A-type unit by an angle of $\frac{\pi}{2}$. C-type arises from clockwise rotation of B-type unit and D-type arises from clockwise rotation of C-type unit, all of them again by $\frac{\pi}{2}$-rotation, respectively. The same procedure of the 3D $\rightarrow$ 2D transformation[b] of the growth unit we have applied in the case of the mutant variant, but now the front and the rear walls of the box are not devoid of H-type monomers but include the smallest number of them. A chemical difference between a non-mutant and mutant variant of lysozyme lies in the D67H mutation[2]. The proteins, which are afflicted with this mutation, have a substitution of aspartate 67 to histidine (D67H) relative to the wild-type (non-mutant) protein. The crystal structure of D67H reveals that the mutation disrupts a series of hydrogen bonds in the β-domain, resulting in a movement of the β-sheet residues and the long loop containing residues 66-74. This is a region of substantially increased mobility, for more details see Refs. [20, 21] and refs therein. These structure perturbations manifest themselves in the properties of the walls of the growth units.

2.2. *Initial surface preparation*

To prepare a good enough, essentially thermodynamically stable (ripe) nucleus we have to check what configuration of the growth units gives the structure with a

[b]For several reasons we claim that the second-stage of the coarse-graining applied allows to perform an interesting and useful 2D model study of the process (see, the Text) but from now on one can try to perform a purely 3D modeling as well. We, however, wish to confine ourselves to the one presented in this paper. Some physically argumented motivations for performing a purely $2D$ modeling, preferentially towards speeding up the process and achieving an optimal (nanotechnological) fabrication of the Langmuir-Blodgett template, one can find elsewhere[19].

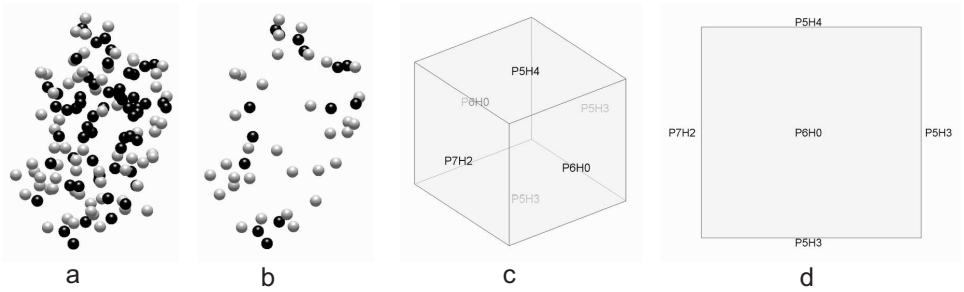

Fig. 2. The growth unit preparation process for the non-mutant variant: a) 3D HP representation of the selected molecule. Black balls represent H-type amino-acids whereas gray balls represent P-type amino-acids. b) Isolated surface (skin) of the molecule. c) 3D cubic representation. The net excess in a number of one of the monomer types determines the type of the wall (side) of the box. d) A 2D growth unit of A-type, see text for better definitions of the cubic (c) and the square boxes (d).

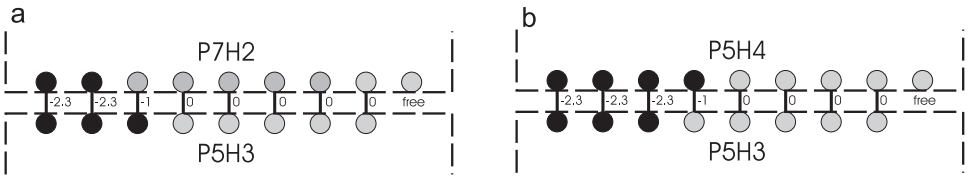

Fig. 3. a) An example of some reciprocal configuration of the two growth units for the non-mutant variant. b) The most frequent reciprocal configuration of the two growth units for the non-mutant variant. Black circles represent H-type amino-acids whereas gray circles represent P-type amino-acids.

minimum energy. To calculate the interaction energy of the two growth units under study we put them in the way that two sides of the non-mutant variant may interact, e.g. P5H3 interacts with P7H2 (see Figure 2d and Figure 3a). It is known from the HP-based "toy brick" model[22] that the interaction energy between monomers of H-type gives $E_{HH} = -2.3$, whereas between monomer of H- and monomer of P-type $E_{HP} = -1$ and between monomers of P-type $E_{PP} = 0$. We have to mention that all values of the interaction energy are given in k_BT units, where k_B - Boltzmann constant and T - the temperature. Because the molecule is flexible, we assume that every possible $H-H$, $H-P$ and $P-P$ bonds are created and the minimum energy of such configuration is equal to a sum of all contact energies, i.e. when P5H3 interacts with P7H2 we can observe maximally two $H-H$ bonds, one $H-P$ and five $P-P$ bonds, thus the total energy: $E = 2E_{HH} + E_{HP} + 5E_{PP} = -5.6$. We can see that the minimum energy is for a configuration in which the P5H3 interacts with P5H4, then $E = -7.9$ (see Figure 3b). We repeat this procedure for every combination of A, B, C and D-type of the growth units on the 2×2, 4×2 and 4×4 lattices. In every case of the non-mutant and mutant variants we observed a recurrent structures (elementary cell): $\begin{array}{|c|c|}\hline \mathbf{B} & \mathbf{C} \\ \hline \mathbf{A} & \mathbf{D} \\ \hline \end{array}$ with the energy of $E = -31.6$ for

the non-mutant variant and of $E = -40.8$ for the mutant variant. Thus, at this stage of construction of our computer model one can anticipate quite a large difference in energy values of both protein forms which will result in more prone-to-aggregation behavior revealed by the crystallizing mutant.

Using so obtained elementary cell we build a well ordered and stable nucleus by the mentioned recurrence procedure applied to the cell. Thus, it yields:

					⋮					
	D	A	D	A	D	A	D	A	D	
	C	B	C	B	C	B	C	B	C	
...	D	A	D	A	D	A	D	A	D	...
	C	B	C	B	C	B	C	**B**	**C**	
	D	A	D	A	D	A	D	**A**	**D**	
					⋮					

Such an ordered structure is characteristic of non-Kossel crystals. Non-Kossel crystals are defined as complex structures with several molecules per unit cell in inequivalent positions, e.g. the lysozyme unit cell as it includes four molecules in different positions[16].

2.3. *The procedure of epitaxial (surface) growth*

During the whole course of the simulation we observe exclusively the nucleus' surface and the growth units which are at the surface at each simulation step. In principle, we do not care about the molecules in the bulk what is consistent with the mesoscopic-modeling idea of the electrostatic double layer which surrounds the growing crystal and in which the most important processes seen in terms of surface formation take place[23]. This hint saves the processor time and also speeds up the growth procedure. The number of the free growth units which are present in a given moment at the surface is always considered to be proportional to the molecule concentration in a virtual solution ("bulk"), e.g. for bulk concentration of 6%, statistically 6% of the surface area is occupied by the growth units. In the beginning, a given number of the growth units, with their random orientations (A, B, C or D), is placed by chance at the surface. There is no possibility that two movable growth units were put one over one because we confine our modeling to the one really nearest layer, only. The movement direction of each growth unit placed at the surface is then randomly chosen: go to the left, go to the right, come off the surface or stay at the same location. The movement probability, $p^{(m)}$, is consistent with the Metropolis Monte Carlo acceptance rule(s). This means that downhill transitions that lower the energy are accepted with probability one and uphill transitions with probability proportional to the Boltzmann factor. There is a possibility that two movable growth units will come across each other. In this case, the movement is

possible to occur after consideration of two components of the interaction energy: (i) interaction energy of the growth unit with the crystals surface and (ii) interaction energy of the growth unit with the neighboring movable growth unit(s). This way we can also observe some temporary aggregated forms of the growth units. Every step is a combination of linear transition and rotation, i.e. the growth unit rolls about the surface. The growth unit becomes a part of the crystal when it is situated in a kink position and its orientation suits the other elements of the crystal unit cell[8,10]. Moreover, there is usually a substantial energy barrier. The reason for this barrier is that an exposed edge site has a higher potential than a corner (kink) site because a molecule sitting at an edge site has the smallest number of nearest neighbors. The resulting barrier is called the Ehrlich-Schwoebel barrier. Moreover, the kink site is the smallest potential site on the surface[24]. In the case of energetically favorable move into a kink position and if the growth unit orientation does not suit the other elements of the crystal unit cell the growth unit will not become a part of the crystal. It is because in the case of lysozyme and other molecular crystals molecules occupying different positions are identical, and thus, are characterized by the same chemical potential in solution, vapor or melt. Correspondingly, the crystal should be characterized by one chemical potential averaged over the unit cell[16].

The growth unit that would become a part of the crystal would still have a small chance to detach but only from the kink position. Detachment probability is proportional to the difference of interaction energies between the new and the old positions, namely $p^{(-)} \simeq \exp(-\Delta E/k_B T)$.

The new layer can start growing only when the bottom layer achieves a certain length equal to some λ_0[25]. This is the minimum length for which the next twist of the spiral can arise (see Figure 1).

3. Growth rate evaluation

According to our PDB-based computer model, the evolution of the growing surface is presented in Figure 4 for a few consecutive simulation steps. We can see that a new terrace (next twist of the spiral) starts growing only when the bottom layer is going to achieve a length of λ_0. For a very big lattice and under a certain set of conditions it is possible to observe that the growing surface experiences a lateral leaning. The slope is a lattice-size dependent value and may vary from a value less than one to some tens of angular degrees. The slope will maximally increase to the value characteristic of the slope of the (110) crystallographic face of the tetragonal crystal which is equal to 45 degrees[28].

The growth rate in the direction normal to the surface is calculated as follows[9]

$$V_{gr} = \frac{v_{step} \cdot d}{\lambda_0}, \tag{1}$$

where v_{step} is a step propagation velocity parallel to the step, λ_0 - average distance between two steps and d is a steps height (see Figure 5). To calculate v_{step} we have to know how many time steps per length λ_0, denoted by t_{lay}, we need for building

Table 1. Experimental data[10,25,26,27] and other parameters used in the simulation. They are depicted in such a sequence that first the thermodynamic parameters appear, then some important kinetic and probabilistic, and finally the sizes and lengths relevant for the system description. (Note that the activation energy ΔE is taken the same for both movement as well as detachment probabilities, because it is calculated in the same way for both probabilities - see text and Figure 4 for details.)

lysozyme concentration in solution	$3 \div 12\%$
temperature, T	$280 \div 310K$
viscosity of the lysozyme solution, η	$2.4 \cdot 10^{-3} \frac{kg}{m \cdot s}$
bulk diffusion coefficient of the lysozyme molecule, $D_B^{310K} = \frac{(k_B T)}{6\pi\eta R_H}$	$4.977 \cdot 10^{-11} \frac{m^2}{s}$
surface diffusion coefficient of the lysozyme molecule, $D_S \approx \frac{D_B^{310K}}{100}$	$4.977 \cdot 10^{-13} \frac{m^2}{s}$
time step, $t_{step} = \frac{\langle x^2 \rangle}{4D_S}$	$7.2532 \cdot 10^{-6} s$
movement probability, $p^{(m)}$	$\simeq (-\Delta E \setminus k_B T)$
attachment probability of the well suited growth unit, $p^{(+)}$	1
detachment probability, $p^{(-)}$	$\simeq (-\Delta E \setminus k_B T)$
lysozyme radius, $R_M (= 1/2d)$	$1.61 \cdot 10^{-9} m$
hydrodynamic radius of lysozyme, R_H	$1.9 \cdot 10^{-9} m$
critical radius for lysozyme crystal, R_c	$2.73 \cdot 10^{-8} m$
minimum distance between two steps, $\lambda_0 = 4R_c$	$1.09 \cdot 10^{-7} m$

one layer of the surface. Therefore, a formula for the growth rate of one building layer can be proposed in a simple form

$$v_{step} = \frac{\lambda_0}{t_{lay}}, \tag{2}$$

where $\lambda_0 = N_{lay} \cdot 2R_M$; here N_{lay} is a number of the growth units indispensable to build one layer; for R_M- see Table 1.

In our simulation, we assume that the step height, d, is equal to the diameter of one building unit, i.e. $d = 2R_M$. After some simple algebra we finally may access an exact formula of the growth rate of the one layer

$$V_{gr_{lay}} = \frac{2R_M}{t_{lay}} \tag{3}$$

and the total growth rate of N layers

$$V_{gr} = \frac{N \cdot 2R_M}{t}, \tag{4}$$

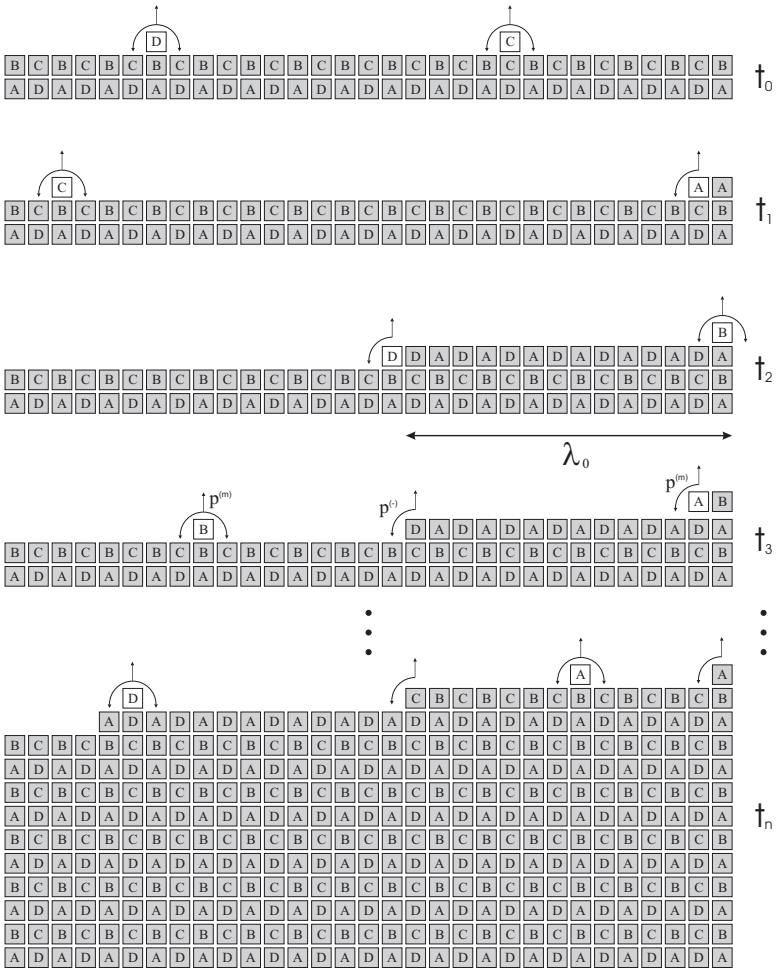

Fig. 4. Consecutive snapshots taken from applying the PDB-based computer model of the growing crystal surface, from top to bottom, in the subsequent simulation steps $t_0 < t_1 < t_2 < t_3 < ... < t_n$. Gray boxes represent the units which already became a part of the crystal, whereas the white ones represent units which may still walk along the crystals surface. Letters signify the growth unit type (see Subsection 2.1 for details). For better visualization λ_0 is taken shorter than in the simulation, cf. Table 1. The presented snapshots are representative of both mutant and non-mutant variants of the studied lysozyme crystal growth.

where N - total number of layers and $t = MCsteps \cdot t_{step}$ is an overall actual time of the simulation, $MCsteps$ - is a total number of steps performed by each growth unit. The time step, t_{step}, of the simulation was calculated to be $7.2532 \cdot 10^{-6} s$ using the equation

$$t_{step} = \frac{\langle x^2 \rangle}{4 D_S}, \tag{5}$$

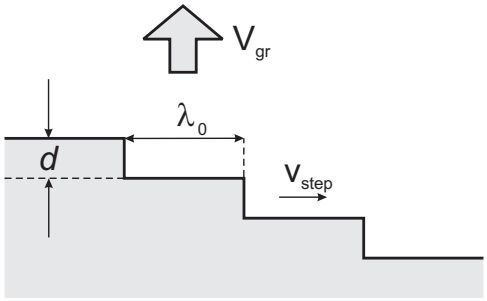

Fig. 5. The vertical cross section of the surface which grows in a spiral mode: This is a key picture to understand that it is legitimate to perform the modeling by its truly $2D$ representation.

where the mean square displacement $\langle x^2 \rangle$, usually evaluated by the second central moment of the probability distribution function $P(x,t)$[29], i.e.

$$\langle x^2 \rangle = \int_0^\infty x^2 P(x,t) dx, \tag{6}$$

was assumed here to be equal to $4R_H^2$, and D_S is a surface diffusion coefficient, see Table 1.

4. Results and discussion

Here one may find an outline of the basic results of our paper, and their discussion, carried out in a systematic way:

A. Figure 6 presents some repeatable tendencies observed while examining the tempo of the formation of mutant vs. non-mutant lysozyme crystal, depending on the lattice size: $30(2R_M) \times 351(2R_M)$ and $50(2R_M) \times 251(2R_M)$, where the first dimension is a lattice height, the second is a lattice width and $2R_M$ is a lattice constant which is equivalent to the size of modeled growth unit. The differences are mostly due to a finite-lattice size effect. The curves have been obtained for the 6% protein concentration. Four regions are depicted on the plot: I – region of pre-nucleational effects. At this stage the first growth units try to join the crystal surface. We can see that the growth rate fluctuations are very strong and the growth rate increases very fast with the increasing number of new terraces. II – region of nucleus formation. At this stage the number of terraces tends to a constant value and depends on the lattice size. III – region of non-stationary crystal growth. At the end of this stage the number of terraces is fixed and is approximately equal to $h = (\text{lattice width})/\lambda_0$. IV – region of stationary, nearly constant-tempo crystal growth. A constant-growth rate of lysozyme crystals is consistent with experimentally observed behavior of lysozyme crystals growth from aqueous solutions[30]. Based on this result, we can conclude that the growth of lysozyme is controlled by the incorporation of lysozyme molecules to the surface of the crystal. In other words,

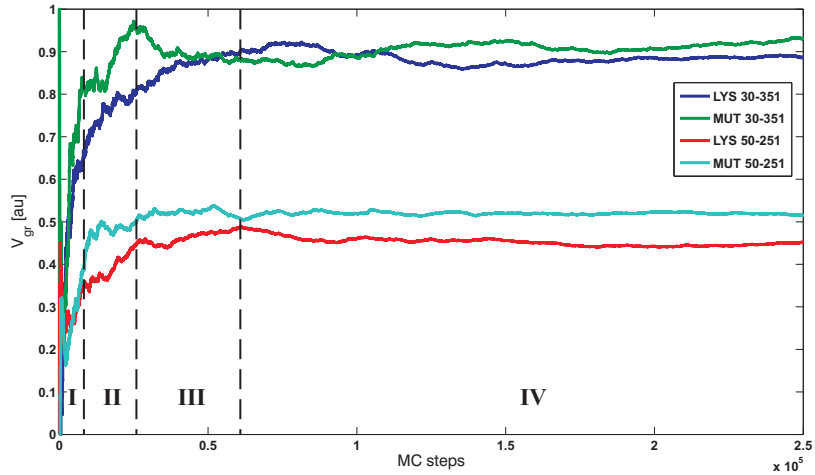

Fig. 6. Some repeatable tendencies observed while examining the tempo of the formation of mutant vs. non-mutant lysozyme crystal, depending on the lattice size: $30(2R_M) \times 351(2R_M)$ and $50(2R_M) \times 251(2R_M)$, cf. Table 1. Four regions are depicted on the plot: I – region of pre-nucleational effects, II – region of nucleus formation, III – region of non-stationary crystal growth, IV – region of stationary, nearly constant-tempo crystal growth. The differences are mostly due to a finite-lattice size effect. The curves have been obtained for the 6% protein concentration which is noticed to show optimal growing aggregation-oriented tendencies for both protein forms under study.

the overall crystal formation has been mainly designed as an interface-controlled phenomenon. Investigations on several types of proteins (insulin, canavalin, and lysozyme) performed by other researchers[31,32] have also suggested that the growth of such proteins is limited by interface-involved rather than by volume transport.

B. Figure 7 presents a comparative plot, roughly revealing three regions of temperature behavior seen in terms of the tempo of the growing (poly)crystalline aggregates for the set of protein concentrations: 3, 6, 9, 12%. Several regions viz parametric windows have been found: I - Region below an optimal temperature for a given lysozyme concentration. In this range of temperature values the growth rate increases with increasing temperature. This behavior is associated with increasing mobility of the growth units but the temperature is still too small for dissolving effects to enter. II – Crystallization window. In this range of temperature values the growth rate conforms to an approximately constant value and the acts of attachment/detachment are balanced. A deflection point is only seen for the non-mutant; the mutant expresses a certain resistance against smooth crystallization and the deflection point is hardly visible for it. III - Region above an optimal temperature for a given lysozyme concentration. In this range of temperature the growth rate is decreasing because detachment starts dominating over the attachment. Outside the window for both variants one detects the protein aggregates that are present

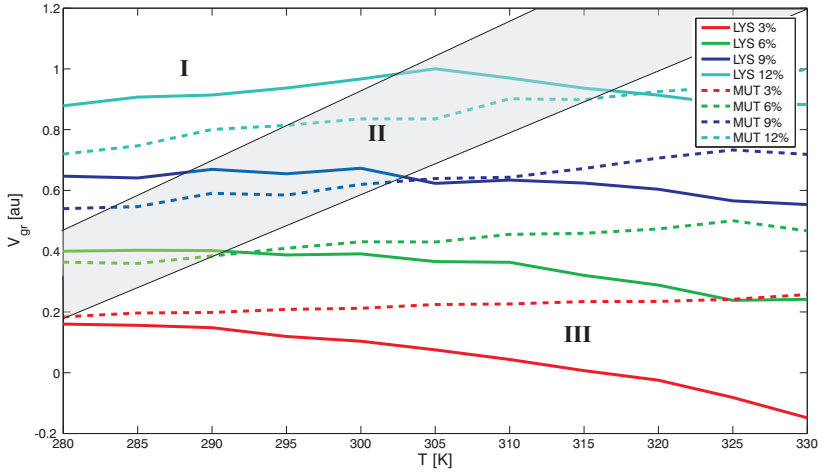

Fig. 7. A comparative plot, crudely revealing three regions of temperature behavior seen in terms of the tempo of the growing (poly)crystalline aggregates for the set of protein concentrations: 3, 6, 9, 12%. I - region below an optimal temperature for a given lysozyme concentration, II – crystallization window, III - region above an optimal temperature for a given lysozyme concentration.

for each of the concentration value chosen.
A tendency of dissolving the crystal appears too - see the lowest curve (LYS 6%) with $V_{gr} < 0$ (due to enormous evaporation).

C. Figure 8 presents a relative surface perturbation h/R as a function of R for different surface lengths $n \times \lambda_0$, where h - height, in principle the number, of terraces, λ_0 - minimum terrace length for which the next terrace can start growing, R crystal height and n - an integer value. It can be seen from Figure 8 that the relative surface perturbation decreases with increasing R and is a strongly lattice-width dependent value. It means, that for the bigger lattice we can obtain higher terraces (in 2D representation) or a spiral cone (in 3D representation). The presented estimate is rather of purely geometrical nature. (It is a question of more reliable and repeatable case-sensitive studies to firmly argue whether or not the perturbation decays in time exponentially fast, as in the M-S linear instability approach to crystal growth[23], or follows some non-exponential decay in time.)

It can be seen from the above that both variants of lysozyme crystallize/aggregate along similar pathways (with similar tendency) but differ from each other in quantitative details, e.g. growth tempo, presence/absence of the deflection point on the diagram, overall design of the below mentioned (morphological) phase diagram of the two lysozyme variants, etc.

A juxtaposition of advantages and disadvantages of the described model is presented below.

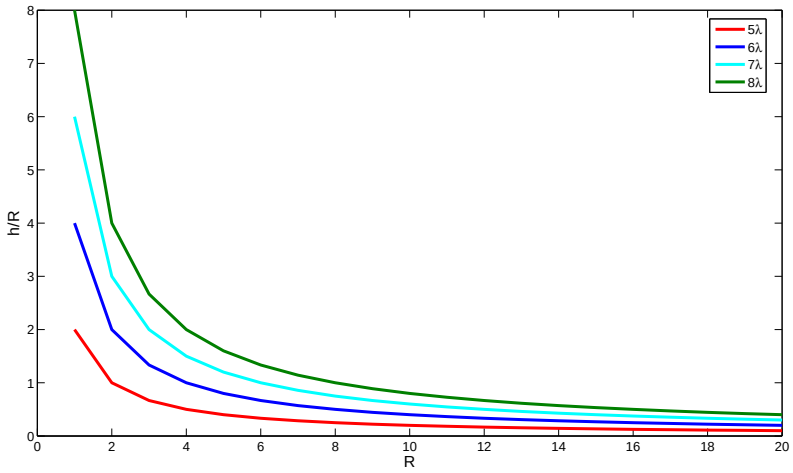

Fig. 8. Relative surface perturbation h/R as a function of R for different surface lengths $n \times \lambda_0$, where h - height, in principle the number, of terraces, λ_0 - minimum terrace length for which the next terrace can start to growth, R crystal height and n - integer value ($n = 5, 6, 7, 8$ appears in the inset of the plot). It can be seen that the relative surface perturbation decreases with increasing R.

(i) Advantages of the model

+ Easy-to-handle implementation of the 3D spiral model of protein crystal growth and aggregation to the 2D simulation can be utilized;
+ Off-lattice preparation of the growth unit basis of the PDB data can be underscored (real interpositions of amino-acids);
+ The obtained unit cells are of non-Kossel type[16] which is characteristic of most of the biomolecular crystals;
+ To calculate the growth rate V_{gr} we used real experimental data, cf. Table 1;
+ It is possible to "control" some of the growth parameters (i.e. solution parameters: ionic strength, pH) by some proper selection of p^+ and p^- values;
+ The offered model tries to capture a from-meso-to-micro passage, quite hardly seen from the platform of a truly mesoscopic crystal-formation model[33];
+ The model is really sensitive to temperature variations[34] which is very important from the point of keeping the crystal formation within a really narrow crystallization (parametric) window[5,15,16], cf. Figure 7;
+ A (morphological) phase diagram in the space of protein concentration (c), temperature (T) and tempo of the growing aggregate (V_{gr}) can also be inferred, cf. Figures 6 and 7 to realize how narrow the crystallization slot

can be, and how vastly the (poly)crystalline, or presumably, amorphous regions of two-variant lysozyme aggregation do arise for different lysozyme concentration values under a certain time (no. of $MCsteps$) vs temperature (T) equivalence principle shown by applying Figures 6 and 7 together, in a form of the common phase diagram.

(ii) Disadvantages of the model

- The coarse-graining procedure of the performed HP-type of modeling (two types of amino-acids: H and P, only three types of possible interactions: $H-H$, $H-P$ and $P-P$) may be anticipated as a certain shortage of the proposed method;
- The model is molecule-orientation dependent; the 3D $\rightarrow$ 2D transformation enforces a certain selection of the direction of observation and it is necessary to neglect two the most nonreactive opposite sides of the 3D growth unit;
- The growth takes place on the lattice and the growth rate appears to be lattice-size dependent, thus our type of modeling may refer likely to a constrained protein crystal growth[35];
- Fairly idealized number of possible bonds between two sides of the growth unit has to be mentioned; we assume that every possible $H-H$, next $H-P$, and finally, $P-P$ bonds are created;
- The crystallization window (optimal 2nd virial coefficient[15,16]), necessary to assure true crystal formation, is somehow enforced by the nature of the model, though some departures from it toward (dis)ordered aggregations can also be foreseen, cf. Figures 6-7 and the discussion on their contents.

5. Conclusions and final remarks

According to our best knowledge, the presented study is a novel realization of the quite well-elaborated and perennially alive problem of non-Kossel crystal growth[15,16,10,11,12].

The basic message coming from our study is that to crystallize the mutant, according to our computer-based protocol, is much harder than doing the same for its non-mutant variant. The reason of such a deficiency is due to different evaporation conditions, and also because the mutant is much more prone to aggregation, also forming fibrils[34] irrespective of the concentration in which the generally (dis)ordered aggregation occurs.

From the performed simulations, with the main result presented in Figures 6 and 7, it is clearly seen that the overall crystal formation process has been mainly designed as an interface-controlled phenomenon[30,36]. The control, or some limitations due to existence of the interface, are imposed on the system when certain random move-attachment-detachment events are going to enter. In our simulation, it is expressed by the (surface) chemical-reaction limit, represented by the corresponding probabilities, $p^{(m)}$, $p^{(+)}$ and $p^{(-)}$, respectively.

Although random move-attachment-detachment events are expected to manifest

readily in the biopolymeric solution[36,29], there is also an evidence[13] that they might change the interface control because there is a different barrier-to-incorporation for monomers when compared with the same type characteristics for their usually heavier (or bigger) aggregating counterparts. Thus, aggregates have bigger chance than monomers to meet the interface and to become eventually incorporated by the crystal surface. (Unfortunately, they also have a real chance to spoil the crystal structure after being incorporated in it.) As a consequence, they may have a certain quite strong impact on the interface behavior. It then leads to the assertion, that the crystal growth most likely takes place under mixed control, see Refs. [7, 16, 15]. For a description of the external-field controlled crystal formation, with some involvement of aggregates, see Ref. [29].

In our model we give a favor to the interface control more visibly than to some external-field control. If the external-field control were based upon emergence of aggregating units in the solution, which is possible, e.g. under some high concentration of the solution[11,15,30], our model would likely fail. Having, however, the detachment probability being somehow, e.g. pH (or salt concentration)-dependent, we would be able to mimic the aggregation effects, changing $p^{(+)}$ or/and $p^{(-)}$ accordingly during computer experiment. If such a variation procedure is being effectively applied, we may switch between a hydrodynamically stable stationary mode, with V_{gr} →const., or may be able to enter one of non-stationary (and unstable from the hydrodynamic point of view[14]) regimes, which results in going outside the kinetic limit of V_{gr} →const., toward a phase separation process. Both situations mentioned are fairly justified from the experimental point of view, cf. Refs. [13, 16, 15], and can also be reproduced by the proposed Monte Carlo model. Maybe, the "integrated"[30] external-field and interface control is best achievable by some model analytic studies, such as those offered in terms of nonequilibrium statistical thermodynamics of mesoscopic type, cf. Refs. [33, 23, 37] and refs therein. In those studies the Boltzmann type and interface-characteristic dependent free energy of the crystallizing system clearly involves a signature of the interface control, while the overall diffusion function refers most probably to an external-field controlling (diffusion) factor. In Refs. [33, 23] some most important physico-chemical circumstances, and their usually stochastic background, toward obtaining $V_{gr} \to const.$ have been thoroughly discussed. A reliable reference to the spiral mode has also been offered therein, see Refs. [33, 23] and refs therein.

Moreover, the first-stage of the coarse-graining procedure, mentioned in Section 1, points readily to our mesoscopic procedure and refers somehow to some analytical studies performed[33,38]. This manifests itself in some elimination of irrelevant stochastic (dynamic) variables such as, e.g. biomolecule atomic details. We focus one's attention, only, on the biomolecule surface and its properties imposing on the growth unit (see Subsection 2.1) which finally determine the properties of the crystal surface (see Subsection 2.2). We can compare this procedure to the peeled building blocks with "reactive" surface, cf. Sections 1 and 2, and Figure 2, on which

the whole "house" (=our crystal) is constructed.

A possible future task can involve some more realistic situations that will exploit a presence of kinetic obstacles, such as mesoscopic impurities, that impede the advancement of crystal front, and that can change the final (poly)crystalline outcome[39,40]. Thus, one may hope for offering such a study based, in principle, on a more realistic biomolecule representation (taken directly from the experimentally motivated and widely available protein data source[2]), departing markedly from its typically used spheroidal counterpart that was applied in Ref. [36].

Acknowledgments

This work is supported by a KBN grant no. 2 PO3B 032 25. A part of this work has been presented by the first author at the "Joint Meeting of German and Polish Associations for Crystal Growth", 6-8 March 2006 Berlin. We thank Dr. Christine B. Trame (Lawrence Berkeley National Laboratory) for her critical reading of this paper.

References

1. R. I. Dima, D. Thirumalai, Protein Sci. **11**, 1036 (2002).
2. The RCSB Protein Data Bank, www.rcsb.org, accesible on the day of writing the paper.
3. K. F. Lau, K. A. Dill, Macromol. **22**, 3986 (1989).
4. J. R. Banavar, M. Cieplak, A. Maritan, Phys. Rev. Lett. **93**, 238101 (2004).
5. D. Thirumalai, D. K Klimov, R. I. Dima, Curr. Opin. Struct. Biol. **13**, 146 (2003).
6. R. G. Larson, L. E. Scriven, H. T. Davis, J. Chem. Phys. **83**, 2411 (1985).
7. A. Pimpinelli, J. Villain, *Physics of Crystal Growth* (Cambridge University Press, New York, 1998).
8. W. K. Burton, N. Cabrera, F. C. Frank, Phil. Trans. Roy. Soc. A **243**, 299 (1951).
9. X. Y. Liu, E. S. Boek, W. J. Briels, P. Bennema, Nature **374**, 342 (1995).
10. A. M. Kierzek, P. Pokarowski, P. Zielenkiewicz, Biophys. Chem. **77**, 123 (1999); A. M. Kierzek, P. Pokarowski, P. Zielenkiewicz, Biophys. Chem. **87**, 43 (2000); A. M. Kierzek, P. Zielenkiewicz, Biophys. Chem. **91**, 1 (2001).
11. A. Nadarajah, E. L. Forsythe, M. L. Pusey, J. Cryst. Growth **151**, 163 (1995); M. Li, A. Nadarajah, M. L. Pusey, J. Cryst. Growth **156**, 121 (1995).
12. M. Ataka, Prog. Crystal Growth Charac. **30**, 109 (1995).
13. S. C. Ke, L. J. DeLucas, J. G. Harrison, J. Phys. D: Appl. Phys. **31**, 1064 (1998).
14. S. Bastea, S. Puri, J. L. Lebowitz, Phys. Rev. E **63**, 041513 (2001).
15. P. Vekilov, J. I. D. Alexander, Chem. Rev. **100**, 2061 (2000).
16. A. A. Chernov, J. Mat. Sci.: Materials in Electronics **12**, 437 (2001).
17. J. Siódmiak, J. Cryst. Growth - submitted.
18. Ch. Wandrey, *Molecular Basis of the Structure and Behavior of Polymers* (École Polytechnique Fédérale de Lausanne, 2003).
19. E. Pechkova, S. Fiordoro, D. Fontani, C. Nicolini, Acta Cryst. D **61**, 809 (2005).
20. A. K. Chamberlain, V. Receveur, A. Spencer, C. Redfield, C. M. Dobson, Protein Sci. **10**, 2525 (2001).
21. K. Takano, J. Funahashi, K. Yutani, Eur. J. Biochem. **268**, 155 (2001).
22. J. Yong-Yun, L. You-Quan, M. Jun-Wen, T. Xiao-Wei, http://arxiv.org/abs/q-bio/0506012, accesible on the day of writing the paper.

23. A. Gadomski, J. Siódmiak, Cryst. Res. Technol. **37**, 281 (2002).
24. R. L. Schwoebel, E. J. Shipsey, J. Appl. Phys. **37**, 3682 (1966).
25. J. Żmija, *Foundations of the theory of crystal growth* (PWN, Warszawa, 1987) - in Polish.
26. D. Lima, A. De Wit, Phys. Rev. E **70**, 021603 (2004).
27. S. Ravichandran, J. Talbot, Biophys. J. **78**, 110 (2000).
28. P. Politi, J. Krug, Surf. Sci. **446**, 89 (2000).
29. A. Gadomski, J. Łuczka, J. Mol. Liquids **86**, 237 (2000).
30. M. Pusey, R. Neumann, J. Cryst. Growth **76**, 593 (1986).
31. E. Forsythe, M. L. Pusey, J. Cryst. Growth **139**, 89 (1994).
32. L. A. Monaco, F. Rosenberger, J. Cryst. Growth **129**, 465 (1993).
33. A. Gadomski, J. Siódmiak, Phys. Stat. Solidi (b) **538**, 242 (2005).
34. L. N. Arnaudov, R. de Vries, Biophys. J. **88**, 515 (2005).
35. W. A. Tiller, J. Cryst. Growth **76**, 607 (1986).
36. S. D. Durbin, G. Feher, J. Cryst. Growth **110**, 41 (1991).
37. J. T. W. M. Tissen, J. G. E. M. Fraaije, J. Drenth, H. J. C. Berendsen, Acta Cryst. D **50**, 569 (1994).
38. A. Gadomski, J.M. Rubí, Chemical Physics **293**, 169 (2003).
39. N. Vandewalle, M. Ausloos, R. Cloots, J. Crystal Growth **197**, 317 (1999).
40. M. Brunsteiner, A. G. Jones, F. Pratola, S. L. Price, S. J. R. Simons, Cryst. Growth Des. **5**, 3 (2005).